

Research Article

ADSORPTION OF A BASIC ORGANIC DYE METHYLENE BLUE FROM AQUEOUS SOLUTION ONTO A LOW-COST BIO SORBENT MADE FROM PEANUT (*ARACHIS HYPOGAEA*) SHELLS

*Anatole KIA MAYEKO KIFUANI, EnochMASIVI NKIAMBBI, Kifline MILEBUDI KIFUANI, Bernick WEMBOLOWA TSHENE and Emmanuel ORIA MATESSO

Laboratory of Physical Organic Chemistry, Water and Environment, Department of Chemistry and Industry, Faculty of Sciences and Technology, University of Kinshasa, P.O. Box 190 Kinshasa XI, Democratic Republic of Congo

Received 11th August 2024; Accepted 15th September 2024; Published online 29th October 2024

Abstract

Organic dyes are among the refractory and persistent pollutants of water. Methylene blue (MB) is one of the organic dyes widely used in the textile and other industries. In this study the removal of methylene blue in aqueous solution was studied by adsorption using a biosorbent prepared from peanut (*Arachis hypogea*) shells (AHB). After characterising the biosorbent, the adsorption tests were carried out in batch tests by varying the following parameters: mass of the biosorbent, contact time, initial concentration and pH of methylene blue solution. The results obtained show that the AHB biosorbent has a pH_{ZPC} of 6.74, a specific surface area of $55.96 \text{ m}^2 \text{ g}^{-1}$ and a maximum observed adsorption capacity (Q_{mo}) of 19.95 mg/g . The maximum adsorption capacity of AHB decrease from 46.50 mg/g to 4.62 mg/g when the amount of the biosorbent increases from 10 g to 1000 g ; in the other hand, the maximum adsorption capacity increases from 9.30% to 92.4% with the increasing of the mass of the biosorbent. The optimal adsorption weight was evaluated to be 800 mg , with a % *Ads* of 89.12% at pH 10, after 210 min. The results obtained show an increase in the maximum adsorption capacity and the maximum adsorption percentage of the biosorbent with the AHB-MB contact time and pH solution and tend to constants. The modeling of the kinetic and equilibrium of adsorption shows that the pseudo-first-order kinetic model ($R_g^2=0.9536$) and the Freundlich equilibrium model ($R_g^2=0.9466$) are better suited to describe the adsorption of MB on AHB compared to the pseudo-second-order kinetic model ($R_g^2=0.9009$) and the Langmuir model ($R_g^2=0.8903$). Adsorption is therefore governed by the attachment of the MB particles to the surface of AHB and occurs through the formation of multilayers. The values of R_L and $1/n$ lower than 1 indicate that the adsorption of MB on the AHB biosorbent is favorable. This suggests that biosorbent from peanut shells is effective for the removal of organic dyes from wastewater.

Keywords: *Arachis hypogea*, Methylene blue, Adsorption, Biosorbent, Kinetic, Isotherm.

INTRODUCTION

Organic dyes represent a wide range of synthetic compounds used for different types of applications. They are used for dyeing textiles, cotton, paper, wood and silk. The annual global production is estimated at 700000 tonnes, of which 140000 are released into effluents during production or use. These organic discharges pose double environmental problem on an aesthetic level (detection from $0,005 \text{ mg/L}$) and with regard to their potential toxicity on aquatic species and humans. Methylene blue is one of the dyes widely used in the textile industry (Pathiana *et al.*, 2017; Jia *et al.*, 2018, Kifuani *et al.*, 2018a). It can inductive various diseases by contact, inhalation or ingestion, including burning sensations in the mouth, nausea, vomiting, diarrhea, gastroenteritis, perspiration, cold sweats, permanent injury to the eyes of humans and animals. The removal of methylene blue and other organic dyes from effluents such as wastewater is important for environmental and human health (Rahimian and Zarinabadi, 2020; Nyakairu *et al.*, 2024). Several methods have been developed for dyes removal classified into biological, chemical and physical methods, including a variety of techniques such as: adsorption, advanced oxidation, biosorption, chemical and electrochemical oxidation, coagulation, filtration, flocculation, Fenton electron process, microbial and fungal decolorization,

photocatalysis, nanofiltration, ozonation, reverse osmosis (Kifuani *et al.*, 2018b; Mekky *et al.*, 2020; Basma *et al.*, 2023; Raiyyaan *et al.*, 2024). The majority of organic dyes are persistent and refractory to wastewater treatment methods. Vanessa *et al.* (2017), Ali *et al.* (2021), Thiene *et al.* (2024) reported that many of these techniques have proven to be expensive or responsible for the pollution induced because of the degradation products formed, sometimes more toxic than the initial dyes themselves. Razia *et al.* (2022), Nadew *et al.* (2023) reported that of all these methods, adsorption was found to be effective in removing organic dyes from wastewater and activated carbon being the most effective adsorbent, but the high cost of its production and difficult regeneration makes it less accessible. Nowadays, biomass from agricultural waste is being tested as low-cost and available biosorbent for the removal of organic dyes from water (Mekhalef *et al.*, 2018; Le *et al.*, 2021; Imram *et al.*, 2022; Jan *et al.*, 2022). These include the biomass of rattan sawdust, apricot stones, banana pith, coconut coir dust, cotton stalk, hazelnut shell, coffee residue, coir pith stone, green pea peels, groundnut shells, mango leaves, mango seed kernel, oil palm shell, orange peel, peach stones, sugarcane bagasse, sunflowers stalks, yellow passion fruit waste, *Curcumeropsismanni* shells, *Hevea brasiliensis* seed coat, *Manihot esculanta* kernels. These materials contain organic substances such as polyphenols, lignin, tannins, pigments and protein which provide surface functions, such as carboxylic acid, ketone, aldehyde, phenol, polyphenols, lactone, pyrone, responsible for the adsorption of organic compounds or other pollutants on their surface (Jia *et*

*Corresponding Author: Anatole KIA MAYEKO KIFUANI,

Laboratory of Physical Organic Chemistry, Water and Environment, Department of Chemistry and Industry, Faculty of Sciences and Technology, University of Kinshasa, P.O. Box 190 Kinshasa XI, Democratic Republic of Congo.

al., 2018; Kifuani *et al.* 2018a; Mobolaji *et al.*, 2021; Hatiya *et al.*, 2022; Basma *et al.*, 2023 ; Gani *et al.*, 2023 ; Gajendiran, 2024; Saad *et al.*, 2024;Thiene *et al.*, 2024). In this study, peanut (*Arachis hypogea*) shells powder, a low-cost and available material, was used as biosorbent to evaluate its ability to removal methylene blue from aqueous solution. The effects of different adsorption parameters were studied including dose of adsorbent, contact time, initial concentration and pH of methylene blue solution.

MATERIELS AND METHODS

Adsorbent preparation

The biomass of *Arachis hypogea* shells was used for the preparation of the biosorbent. The sample was collected in the city of Mbanza Ngungu, Province of Kongo Central, Democratic Republic of Congo. The peanut shells were first washed with distilled water, dried in an oven at 105°C (DESPATCH Oven Co, type Elect), crushed (Thomas, Type Elect) and then sieved to obtain a fine powder ($\leq 500 \mu\text{m}$). The *Arachis hypogea* biosorbent (AHB) thus obtained were stored in a desiccator at laboratory temperature (28°C), to keep it free from moisture contact and oxidation (Kifuani *et al.*, 2018a).

Adsorbent characterization

The biosorbent was characterized by the determination of physicochemical parameters including Humidity, Dry matter, Ash, pH_{ZPC} and Specific surface area.

Humidity and dry matter

Humidity (H) and dry matter (DM) were determined by volatilization gravimetry using 5 g of biosorbent AHB, heated in an oven. Equation 1 was used to calculate the humidity level (%H) (Ajala *et al.*, 2024):

$$\%H = \frac{(m_1 - m_2) \cdot 100}{m_1} \quad (1)$$

Where, m_1 and m_2 , the weights of biosorbent before and after steaming, respectively.

The dry matter level (%DM) was determined after deducting the humidity level from 100% of the initial sample.

Ash content

The ash content was determined by calcining 5 g of biosorbent in a muffle furnace (NABER, Model N7/H) for 8 hours and calculating the mass loss of the sample. The ash content (%A) of the biosorbent was determined using the following equation2 (Basma *et al.*, 2024):

$$\%A = \frac{(m_3 - m_4) \cdot 100}{m_3} \quad (2)$$

Where, m_3 and m_4 , the weights of biosorbent before and after calcination, respectively.

Determination of pH_{ZPC}

The pH_{ZPC} (pH of zero point of charge) was determined by the pH drift method using 100 mL of 0.01 mol L⁻¹ NaCl solutions

placed in different Adsorbers (LACOPE ADX).The pH of these solutions was adjusted from 2 to 12, by addition of 0.1 N HCl or 0.1 N NaOH solutions, to adjust the acidic or basic solutions, respectively. 1000 mg of biosorbent are then added to each solution and the suspension was stirred for 72 h and centrifuged at 3000 rpm (Centrifuge Labofuge 200 Heraeus). The final pH of each solution was determined using a pH-meter (Hanna Instruments). The pH_{ZPC} is given by the intersection of the curve obtained by plotting the final pH as a function of the initial pH of each solution (Kifuani *et al.*, 2012; Musah *et al.*, 2020).

Determination of specific surface area

The Kifuani volume variation method (KVVM) was used to evaluate the specific surface area of the biosorbent. This method consists of studying, at equilibrium time, the adsorption of methylene blue with a low weight of biosorbent (5 mg) using increasing volumes (100 mL to 1000 mL) of MB solutions (50 mg L⁻¹). The Gaussian curve obtained by plotting the adsorption capacity (q_e) of the biosorbent as a function of the volume (V) of MB solution, allows, through the plateau, to determine the maximum adsorption capacity (q_m) corresponds to the maximum observed adsorption capacity (q_{mo} or Q_{mo}) (Kifuani *et al.*, 2012; Kifuani, 2013; Kifuani *et al.*, 2018a). The specific surface area (S_{MB}) is then calculated according the following equation (Kifuani *et al.*, 2012):

$$S_{\text{MB}} = Q_{\text{mo}} \cdot N_A \cdot s \quad (3)$$

Where, S_{MB} being the specific surface area determined using MB as adsorbate (m² g⁻¹), Q_{mo} the maximum observed adsorption capacity (mg g⁻¹), N_A the Avogadro number (6.022 10²³ mol⁻¹) and s , the area occupied by a MB molecule (175 Å²).

Adsorbate and adsorbate solutions

Methylene blue, a cationic thiazine dye, was used in this study as a model of organic dye and also it is recommended for the characterization of adsorbents. Its IUPAC name is 3,7- Bis (dimethylamino) phenothiazin- 5- ium chloride. Its chemical formula is C₁₆H₁₈N₃SCl and Mw 319.852 g mol⁻¹. It has a flat surface of 175 Å². Methylene blue used in this study was obtained from Merck and used without purification. All the reagents used in this study were of analytical grade. The chemical structure of MB is given by Figure 1.

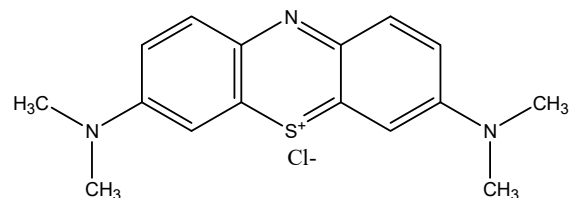


Figure 1. Structure of Methylene Blue

Methylene blue solutions were prepared by dissolving MB crystals in distilled water and diluting the resulting solution to obtain solutions ranging from 1 mg L⁻¹ to 100 mg L⁻¹. The pH of the MB solutions was adjusted by adding 0.1 N HCl or 0.1 N NaOH solutions to obtain solutions ranging from pH 3 to 12. The MB solutions, before and after adsorption, were analyzed using a UV-Vis spectrophotometer (HACK Spectrophotometer, SP, model 1105) at maximum length wave for each pH. The

Beer-Lambert equation was used to calculate the residual concentration of the MB solution (Raiyyaan *et al.*, 2021):

$$A = \varepsilon.l.C \quad (4)$$

With, A being the absorbance, ε the molar absorption coefficient ($L\ mg^{-1}\ cm^{-1}$), l the thickness of the cell (1cm) and C , the concentration of the solute ($mg\ L^{-1}$).

Batch adsorption experiments

The adsorption tests were carried out in static regime in adsorbers (LACOPE ADS) by varying the following parameters: mass of the biosorbent, concentration and pH of MB solution and the contact time. The masses of the biosorbent were varied from 10mg to 1000 mg, the concentration of the MB solution from $1\ mg\ L^{-1}$ to $100\ mg\ L^{-1}$ and the contact time was from 0 to 390 minutes. The pH of the solutions was from 3 to 12. Before use, the AHB biosorbent was dried in an oven at $105^\circ C$ for 3 h and the mass of the biosorbent was determined by weighting using an analytical balance (HEB-E 303). The adsorption tests were carried out with 100 mL of MB solution and the required mass of biosorbent. After stirring for the required time, the suspension was centrifuged at 3000 rpm for 30 minutes and the supernatant was analyzed with a UV-Vis spectrophotometer at the appropriate wavelength, to determine the residual concentration of MB solution. Each experiment is repeated three times to determine the absolute error. The adsorption capacity (Q_e) and adsorption percentage (%Ads) were calculated using equations 5 and 6 (Mobalaji *et al.*, 2021):

$$Q_e = \frac{(C_o - C_e)V}{m_B} \quad (5)$$

$$\% Ads = \frac{C_o - C_e}{C_o} \times 100 \quad (6)$$

With, Q_e being the apparent adsorption capacity or the equilibrium capacity of the biosorbent ($mg\ g^{-1}$), C_o the initial concentration of methylene blue solution ($mg\ L^{-1}$), C_e the residual or equilibrium concentration ($mg\ L^{-1}$), V the volume of the methylene blue solution (L) and %Ads, the adsorption percentage.

Adsorption kinetics

The modeling of the adsorption kinetic was done according to Lagergren kinetic model (Mekky *et al.*, 2020) using the kinetic equations of the surface reaction of pseudo-first-order and pseudo-second-order developed by Kifiani (Kifiani *et al.*, 2012; Kifiani, 2013):

Kifiani Pseudo-first-order kinetic model:

$$\ln \frac{q_e}{(q_e - q_t)} = k_1 t \quad (7)$$

With, q_e being adsorption capacity at equilibrium ($mg\ g^{-1}$), q_t adsorption capacity at time t ($mg\ g^{-1}$), $q_e - q_t$ adsorption capacity of free sites, t the time (s) and k_1 , the constant rate of pseudo-first order reaction (min^{-1}). The plot of $\ln \frac{q_e}{(q_e - q_t)}$ versus t

gives a line whose slope corresponds to k_1 , the rate constant of pseudo-first-order reaction.

Kifiani Pseudo-second-order kinetic model:

$$\frac{q_t}{q_e(q_e - q_t)} = k_2 t \quad (8)$$

Where, k_2 is the rate constant of the pseudo-second-order reaction ($g\ mg^{-1}\ min^{-1}$). The plot of $\frac{q_t}{q_e(q_e - q_t)}$ versus t , gives a line whose slope corresponds to k_2 , the rate constant of the pseudo-second-order reaction.

Adsorption isotherms

The modeling of the adsorption isotherms was carried out for solutions with pH of 3 to 12 using the Langmuir and Freundlich equilibrium models given by the following equations (Alouani *et al.*, 2018):

Langmuir model:

$$\frac{1}{Q_e} = \frac{1}{Q_m} + \frac{1}{Q_m K_L} \cdot \frac{1}{C_e} \quad (9)$$

Where, Q_e is the apparent adsorption capacity of the biosorbent ($mg\ g^{-1}$), Q_m the adsorption capacity at saturation or maximum adsorption capacity ($mg\ g^{-1}$), K_L equilibrium constant adsorption ($L\ mg^{-1}$) and C_e , equilibrium concentration.

The plot of $1/Q_e$ versus $1/C_e$ gives a line which allows to determine Q_m and K_L , from the intercept and slope, respectively.

The Langmuir separation parameter (R_L) was calculated by the following equation (Hajir *et al.*, 2024):

$$R_L = \frac{1}{1 + K_L C_o} \quad (10)$$

With, K_L being the Langmuir constant ($L\ mg^{-1}$) and C_o the initial dye concentration.

Freundlich model:

$$\log Q_e = \log K_F + \frac{1}{n} \log C_e \quad (11)$$

Where, Q_e the adsorption capacity at equilibrium ($mg\ g^{-1}$), K_F the adsorption constant (Freundlich constant), C_e the concentration of the adsorbate at equilibrium ($mg\ L^{-1}$) and n , the Freundlich constant, characterizing the affinity of solute for the adsorbent (affinity parameter). The plot of $\log Q_e$ versus $\log C_e$ gives a line which allows to determine K_F and $1/n$ from the intercept and slope, respectively.

RESULTS

Characteristics of the biosorbent AHB

Table 1 gives the physicochemical characteristics of AHB biosorbent. From these results, it appears that the AHB

biosorbent has an H_{ZPC} of 6.74, a specific surface area (S_{MB}) of $55.69\text{m}^2\text{g}^{-1}$ and a maximum observed adsorption capacity (Q_{mo}) of 19.95mg/g .

Table 1. Parameters in place of Parametres

Paramètres	Values
Particle seize (μm)	≤ 500
Humidity (%)	6.80
Dry matter (%)	92.80
Ash (%)	20.40
pH_{Zpc}	6.74
Q_{mo} (mg g^{-1})	19.95
S_{MB} (m^2g^{-1})	55.69

Effect of biosorbent amount

The results shown in Table 2, Figures 2 and 3 give the effect of the amount of biosorbent on adsorption of BM on AHB biosorbent. Figure 2 shows that the maximum adsorption capacity of AHB decrease from 46.50mg/g to 4.62mg/g when the amount of the biosorbent increases from 10g to 1000g . In the other hand, Figure 3 show an increase of the maximum adsorption capacity from 9.30% to 92.4% with the increasing of the mass of biosorbent. The optimal adsorption weight was evaluated to be 800mg , with a $\%Ads$ of 89.12% and Q_m of 5.32mg/g , after 210min . After this amount of biosorbent, the maximum adsorption capacity and the maximum adsorption percentage tend towards constants.

Table 2. Equilibrium concentration (C_e), maximum adsorption capacity (Q_m), maximum percentage of adsorption ($\%_mAds$), equilibrium time (t_e) at different weights of biosorbent (m_{AHB})

m_{AHB} (mg)	Q_m (mg g^{-1})	$\%_mAds$	t_e (min)
10	46.50	9.30	300
20	34.80	13.92	300
100	24.15	48.30	330
200	15.35	61.39	330
400	10.80	86.40	270
600	7.00	83.96	270
800	5.32	85.12	210
1000	4.62	92.43	210

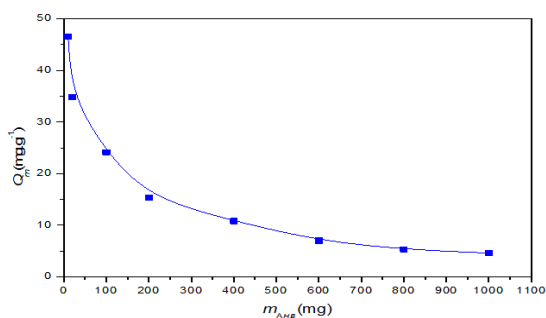


Figure 2. Maximum adsorption capacity (Q_m) vs dose of biosorbent (m_{AHB})

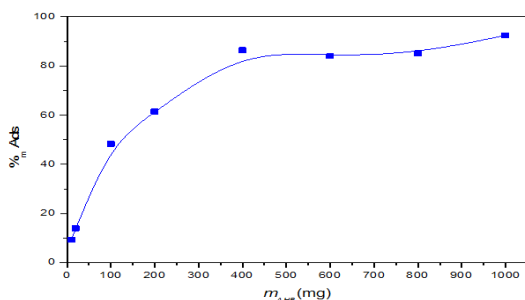


Figure 3. Maximum percentage of adsorption ($\%_mAds$) vs dose of biosorbent (m_{AHB})

Effect of contact time

The results obtained presented in Figures 4 to 7 show an increase in the maximum adsorption capacity and the maximum adsorption percentage of the biosorbent with AHB-MB contact time at different masses of biosorbent and different pH. The optimum equilibrium time is estimated at 300 minutes. The curves obtained by plotting the adsorption capacity or the adsorption percentage vs HAB-MB contact time show three adsorption phases: a first rapid phase at the start of adsorption, followed by a second slow phase and a third adsorption phase during which adsorption is constant.

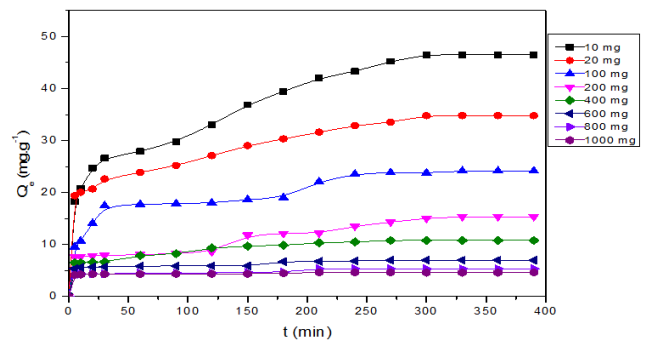


Figure 4. Effect of contact time on adsorption capacity (Q_t) of AHB at different doses of adsorbent

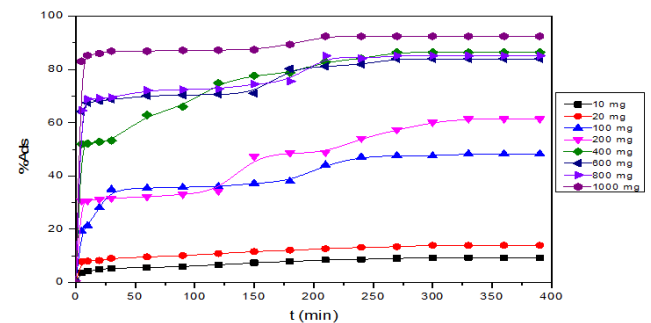


Figure 5. Effect of contact time on the adsorption percentage ($\%Ads$) of AHB at different doses of adsorbent

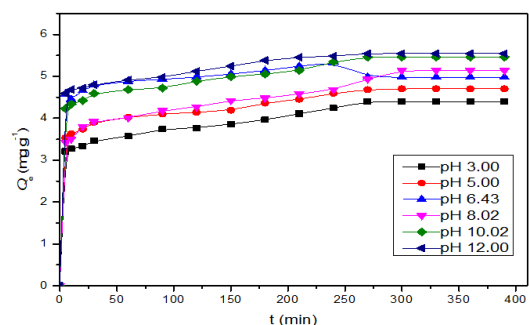


Figure 6. Effect of contact time on the adsorption capacity (Q_t) of AHB at different pH

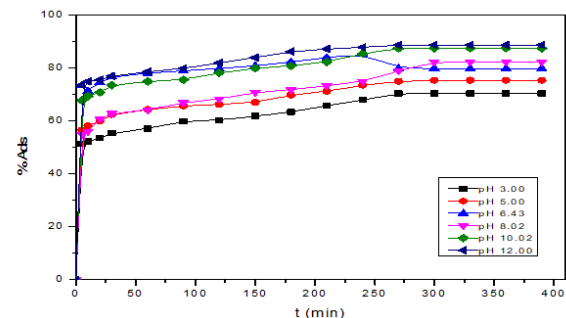


Figure 7. Effect of contact time on the adsorption percentage ($\%Ads$) of AHB at different pH

Effect of initial Methylene blue concentration

The effect of the initial concentration on adsorption was analyzed at different pH (3-13) to obtain the adsorption isotherms. The adsorption isotherms obtained (figures not include) are all of S type.

Effect of pH

The results reported by Table 3 and Figures 8 and 9 show that the maximum adsorption capacity and the maximum adsorption percentage increase from 4.40 mg/g to 5.54 mg/g and from 70.4% to 87.38%, respectively, when the pH of the MB solution increases from 3 to 12. The maximum adsorption capacity and the maximum adsorption percentage are evaluated at 5.46 mg/g and 87.38%, at pH 10, after 270 minutes.

Table 3. Maximum adsorption capacity (Q_m), maximum percentage adsorption ($\%_m Ads$), and equilibrium time (t_e) at different pH

pH	Q_m (mg g ⁻¹)	$\%_m Ads$	t_e (min)
3.02	4.40	70.40	270
5.02	4.70	75.25	270
6.43	4.96	79.75	210
8.02	5.14	82.25	300
10.00	5.46	87.38	270
12.00	5.54	88.63	240

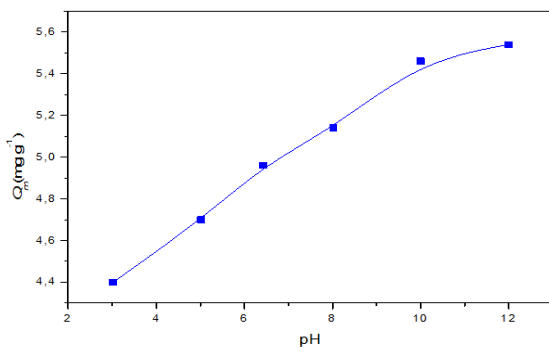


Figure 8. Effect of pH on the maximum adsorption capacity (Q_m) of AHB

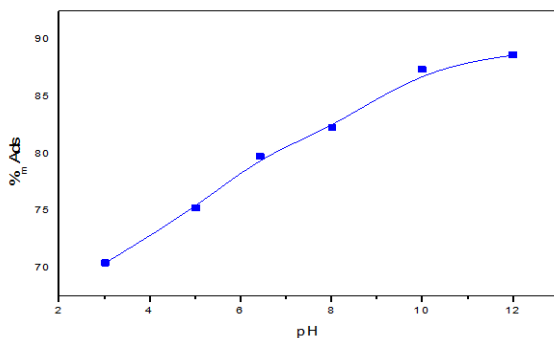


Figure 9. Effect of pH on the maximum adsorption percentage ($\%_m Ads$) of AHB

Modeling of adsorption kinetics

The results of the modeling of the adsorption of MB on AHB according to the kinetic models of pseudo-first-order and pseudo-second order are given in Table 4. These results show that, at different pH, the k_1 constants range from 0.0048 min⁻¹ to 0.2228 min⁻¹, while the k_2 values range from 0.0028 g mg⁻¹ min⁻¹ to 0.0593 g mg⁻¹ min⁻¹.

Table 4. Pseudo-first-order and pseudo-second-order parameters for the adsorption of MB onto AHB at different pH

pH	Pseudo-first-order parameters		Pseudo-second-order parameters	
	k_1 (min ⁻¹)	R^2	k_2 (g mg ⁻¹ min ⁻¹)	R^2
3.02	0.0661	0.9701	0.0026	0.8389
5.02	0.0112	0.9267	0.0593	0.8624
6.43	0.0228	0.9339	0.0035	0.7725
8.02	0.0048	0.9796	0.0029	0.9625
10.00	0.0059	0.9829	0.0028	0.9742
12.00	0.0104	0.9284	0.0032	0.9949
	R^2_g	0.9536		0.9009

Modeling of adsorption isotherms

The modeling of adsorption isotherms according to the Langmuir and Freundlich equilibrium models made it possible to determine the parameters of each model for each pH given in Table 5: Langmuir parameters (Q_m , K_L , R_L) and Freundlich parameters (K_F , $1/n$).

Table 5. Langmuir and Freundlich parameters for the adsorption of MB onto AHB at different pH

pH	Langmuir parameters				Freundlich parameters		
	Q_m (mg.g ⁻¹)	K_L (L.mg ⁻¹)	R_L	R^2	K_f^* (mg.L ⁻¹) ^{-1/n}	$1/n$	R^2
3.02	16.33	0.36	0.0529	0.9193	0.24	0.9562	0.9492
5.02	4.70	0.34	0.0690	0.9240	0.29	0.7412	0.9683
6.43	19.33	0.43	0.0328	0.9102	0.31	0.8757	0.9207
8.02	6.05	0.46	0.0890	0.8515	0.17	0.5440	0.9615
10.02	23.62	0.52	0.0429	0.8479	0.59	0.7448	0.9271
12.02	9.96	0.40	0.0703	0.8903	0.43	0.6272	0.9466
	R^2_g			0.8905			0.9456

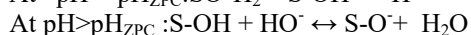
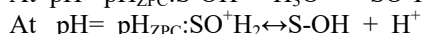
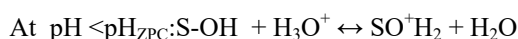
The overall correlation coefficients (R_g^2) of Langmuir and Freundlich models are respectively 0.8905 and 0.9456.

DISCUSSION

The maximum observed adsorption capacity (Q_{mo}) of AHB with a value of 19.95 mg g⁻¹ (Table 1) is lower compared to that reported by Rahimian and Zarinabadi (2020) with 40.0 mg g⁻¹ for the leaves of pine trees biosorbent. The pH_{ZPC} of 6.74 indicates that the surface of the biosorbent is neutral at this pH, positive at a pH < pH_{ZPC} and negative at pH > pH_{ZPC} . The decrease of the maximum adsorption capacity (Q_m) when the mass of the biosorbent increases (Table 2 and Figure 2) is due to the mass effect of the biosorbent, making a certain fraction of the biosorbent unavailable for adsorption but taken into account in the calculation of Q_m . There is molecular steric hindrance. On the other hand, the maximum adsorption capacity increases when the mass of the biosorbent increases (Table 2 and Figure 3) due to the availability of a large number of free active sites. Similar observation was reported by Kifuaniet al. (2018a) in studying the adsorption of methylene blue in aqueous solution on a biosorbent from agricultural waste of *Cucumeropsis mannii* Naudin. These results are also in agreement with those obtained by Razia *et al.* (2022). The increase of the adsorption capacity or the percentage of adsorption of AHB biosorbent with contact time for different masses of biosorbent and pH of methylene blue solution (Figures 4 to 7) is due to the availability of free sites of adsorption with the increase of these parameters (Ajala *et al.*, 2024). The increase in adsorption capacity and percentage of adsorption is rapid in the first phase. This rapid increase is due to the availability of a large number of free sites in the beginning which gradually become saturated to reach the maximum apparent adsorption capacity indicated by a

horizontal line. At this moment the sites are saturated and the adsorption becomes constant. Many other studies have also reported similar results (Nigist *et al.*, 2022; Gani *et al.*, 2023). Musah *et al.* (2020) also reported the same observations on the decrease in the adsorption percentage with the concentration of the solution for the adsorption of methylene blue on a biosorbent from *Platanus orientalis* leaf powder. The S type isotherm obtained for all pH indicate a vertical adsorption of the organic MB cations on the surface of the AHB biosorbent (Kifuani *et al.*, 2012; Razia *et al.*, 2022).

The increase in the maximum adsorption capacity and the maximum adsorption percentage with the pH of MB solution is explained by the surface charge of the biosorbent. The reactions on the surface (S) of the biosorbent are as follows:



At pH = pH_{ZPC} (=6.74), the surface of the biosorbent is neutral. Below the pH_{ZPC} , the surface of the biosorbent is positive, which leads to repulsive interactions between the surface of the biosorbent and the organic cations of methylene blue, hence the reduction in the capacity and percentage of adsorption observed. Beyond the pH_{ZPC} , the surface of the biosorbent is negatively charged, there are then attractive interactions between the surface of the biosorbent and the organic cations which lead to an increase in the capacity and the percentage of adsorption. The optimum pH was set at 10 with maximum adsorption percentage of 87.38% after 270 minutes (Table 3, Figures 8 and 9). The adsorption of MB on the AHB biosorbent is therefore better in a basic medium compared to an acidic medium. These results are in agreement with the work of other researchers for the adsorption of this dye on other adsorbents (Ajala *et al.*, 2024).

The kinetic results (Table 4) show that the overall correlation coefficient of the pseudo-first-order ($R_g^2 = 0.9536$) is higher than that of the pseudo-second-order ($R_g^2 = 0.9009$), which suggests that the pseudo-first-order kinetic model is better suited to describe the adsorption of MB onto the biosorbent. This correlation assumes that adsorption is governed by the attachment of MB particles to the surface of the biosorbent (Kifuani, 2013). This correlation, less than 1, does not exclude other adsorption mechanisms. Similar kinetic results have been reported in the literature (Nadew *et al.*, 2023). The adsorption equilibrium was modelled according to Langmuir and Freundlich equilibrium models (Table 5). The results obtained show that the Freundlich model ($R_g^2 = 0.9466$) is better to describe the adsorption of BM on the biosorbent AHB compared to Langmuir model ($R_g^2 = 0.8903$). The correlation with Freundlich model suggests multilayer adsorption, which appears at high concentrations of MB solution (Kifuani, 2013). This assumes a heterogeneity of the adsorption surface with sites of different adsorption energies (Narayana and Ravi, 2019). Similar results have been reported in the literature (Bharath and Senthil, 2022; Basma *et al.*, 2023; Gani *et al.*, 2023). The equilibrium parameter or separation parameter, K_L , indicates the affinity of the biosorbent towards methylene blue, which can be favorable ($0 < R_L < 1$), irreversible ($R_L = 0$), linear ($R_L = 1$) or unfavorable ($R_L > 1$) (Hajir *et al.*, 2024). The R_L values obtained < 1 , for all pH studied, indicate that the adsorption of MB on AHB biosorbent is favorable (Table 5). The K_F values represent the adsorbent power of the biosorbent,

when the concentration (C_0) of BM is unitary. The Freundlich parameter $1/n$ indicate the adsorption intensity or adsorption interaction strength. It is reported that the adsorption can be favorable ($1/n < 1$), linear ($1/n = 1$), physical and unfavorable ($1/n > 1$) (Basma *et al.* 2024; Hajir *et al.* 2024). The values of $1/n$ lower than 1 suggest that the adsorption of BM on the AHB biosorbent is favorable.

Conclusion

The removal of the organic dye methylene blue in aqueous solution was studied in batch experiments using a biosorbent prepared from peanut shells. The results obtained show that the AHB biosorbent has a specific surface area of $55.69 \text{ m}^2 \text{ g}^{-1}$ and a maximum observed adsorption capacity (Q_{mo}) of 19.95 mg g^{-1} . The optimal condition determined are 800 mg of MB at a pH of 10 with a percentage of adsorption of 87.38% after 270 minutes. Adsorption is a function of the mass of the biosorbent, contact time, pH and initial concentration of MB. Methylene blue elimination is better in a basic medium compared to acidic medium. Adsorption of MB dye on biosorbent AHB is better described by the pseudo-first-order kinetic model and the Freundlich equilibrium model compared to pseudo-second-order kinetic model and the Freundlich equilibrium model. The results obtained in this study show that peanut shells are effective for removal of MB dye from wastewater.

Competing interests: The authors declare that they have no competing interests.

Authors' contributions: All authors contributed to data analysis and discussion of results.

Acknowledgements: The authors of the manuscript gratefully acknowledge Jerry IKELE KURAYUM and Kifline MILEBUDI KIFUANI family for the facilities provided to Professor Anatole KIA MAYEKO KIFUANI, during the final editing of this article in Aurora-Denver, Colorado, USA.

REFERENCES

- Ajala, E.,O., Aliyu, M.,O., Ajala, M., A, Mamba, G, Ndana, A.M., and Olatunde, T.S. 2024. Adsorption of lead and chromium ions from electroplating wastewater using plantain stalk modified by amorphous alumina developed from waste cans. *Scientific reports*, 14:6055. DOI: <https://doi.org/10.1038/s41598-024-56183-2>.
- Ali, K., Javaid, U.,J., Ali, Z., and Zaghum, M.,J. 2021. Biomass-derived adsorbents for dye and heavy metal removal from wastewater. *Adsorption Science and Technology*, 2021:1-14. DOI: <https://doi.org/10.1155/2021/9357509>.
- Alouani, M.E.L., Alehyen, S., Achouri, M.E.L., Taibi, M. 2018. Removal of cationic dye methylene blue from aqueous solution by adsorption on fly ash-based geopolymer. *J. Mater. Envir. Sci.*, 9(1):32-46. DOI: <https://dx.doi.org/10.26872/jmes.2018.9.1.5>.
- Basma, G., Alhagbi, G.S.A. 2023. An investigation of a natural biosorbent for removing methylene blue dye from aqueous solution. *Molecules*, 28(6): 2785. DOI: <https://doi.org/10.3390/molecules28062785>.
- Basma, I.W., Israa, S.A.B., Asrar, A.A. and Marial, A.M. 2024. Adsorption isotherms and kinetics studies of lead on polyacrylonitrile-based activated carbon nonwoven nanofibers. *Ecological Engineering and Environmental*

- Technology*, 25 (6):20-26. DOI: <https://doi.org/10.12912/27197050/186546>.
- Bharath, B.G., and Senthil, P. 2022. Adsorptive Removal of Alizarin Red S onto sulfuric acid modified avocado Seeds: Kinetics, Equilibrium, and Thermodynamic studies. *Adsorption Science & Technology*, 2022:ID3137870. DOI: <https://doi.org/10.1155/2022/3137870>.
- Gani, P., and Puji L. 2023. Comparison of two biosorbent beads for methylene blue discoloration in water. *J. Ecol. Eng.*, 24(8):137-145. DOI: <https://doi.org/10.12911/22998993/166319>.
- Gajendiran, V., Deivasigamani, P., Sivamani, S. and Banarjee, S. 2024. Biochar from Manihot esculenta stalk as potential adsorbent for removal of reactive yellow dye. *Desalination and water Treatment*, 317: 100120. DOI: <https://doi.org/10.1016/j.dwt.2024.100120>.
- Hajir, N., Abdelrahman, B.F., and Oma, A.S. 2024. Isothermal and kinetics investigation of dibenzothiophene removal from model fuel by activated carbon developed from mixed date seed and PET Wastes. *Journal of Ecological Engineering*, 25(3):38–52. DOI:<https://doi.org/10.12911/22998993/177628>.
- Hatiya, N.A., Reshad, A.S. and Negie, Z.W. 2022. Chemical modification of Neem (*Azadirachta indica*) biomass as bioadsorbent for removal of Pb²⁺ ion from aqueous wastewater. *Adsorption Science and Technology*, 2022 :1-18. DOI: <https://doi.org/10.1155/2022/7813513>.
- Imran, M.S., Javed, T., Areej, I., and Haider, M.N. 2022. Sequestration of crystal violet dye from wastewater using low-cost coconut husk as a potential adsorbent. *Water. Sci. Technol.*, 285 (8):2295-2317. <https://doi.org/10.2166/wst.2022.124>
- Jan, S.U., Ahmad, Y., Ali, M, Hussain, Z., and Melhi S. 2022. Adsorptive removal of methylene blue from aqueous solution using sawdust. *Medicom Pharmaceutical Sciences*, 2 (1): 8-16.
- Jia, P., Tan, H, Liu, K., and Gao, W. 2018. Removal of methylene blue from aqueous solution by bone char. *Appl. Sci.*, 1903 :1-11. DOI : 10.3390/app8101903.
- Kifuani, A.K.M., Noki, P.V., Ndelo, J.D.P., Mukana, W.M., Ekoko, G.B., Ilinga, B.L. and Mukinayi, J.M. 2012. Adsorption de la quinine bichlorhydrate sur charbon actif peu couteux à base de la bagasse de canne à sucre imprégnée de l'acide phosphorique. *Int. J. Biol. Chem. Sci.*, 6(3): 1337-1359. DOI: <https://dx.doi.org/10.4314/ijbcs.v6i3.36>.
- Kifuani, A.K.M. 2013. Adsorption des composés organiques aromatiques en solution aqueuse sur charbon actif à base des déchets agroindustriels. Thèse de doctorat, Université de Kinshasa.
- Kifuani, K.M., Kifuani, A.K.M., Ilinga, B.L., Ngoy, P.,B., Monama, T.O., Ekoko, G.B., Mbala, B.M. and Muswema, J.L. 2018a. Adsorption d'un colorant basique Bleu de Methylene en solution aqueuse sur un bioadsorbant issu de déchets agricoles de *Cucumeropsis mannii* Naudin. *Ind . J. Biol. Chem. Sci.*, 12 (1):558-575. DOI: <https://dx.doi.org/10.4314/ijbcs.v12i1.43>.
- Kifuani, K.M., Kifuani, A.K., M., Ilinga, B.L., Ngoy, P.B., Monama, T.O., Ekoko, G.B., and Muswema, J.L. 2018b. Kinetics and thermodynamic studies adsorption of Methylene Bleu in aqueous solution on a bioadsorbent from *Cucumeropsis mannii* Naudin waste seeds. *Ind . J. Biol.Chem. Sci.*, 12 (5): 2412-2423. DOI: <https://dx.doi.org/10.4314/ijbcs.v12i5.38>.
- Le, P.T., Bui, H.T., Le, T., H., Nguyen, T.H., Pham, L.A., Nguyen, H.N., Nguyen, Q.S., Nguyen, T.P., Bich, N.T., Duong, T.T., Herrmann, M., Ouillon and Le, T.P.Q. 2021. Preparation and characterization of biochar derived from agricultural by-products for dye removal. *Adsorption Science and Technology*, 2021:1-21. DOI: <https://doi.org/10.1155/2021/9161904>.
- Mekhalef, B.F., Kacha, S.L.A., and Belaid, K.D. 2018. Étude comparative de l'adsorption du colorant Victoria Bleu Basique à partir de solutions aqueuses sur du carton usagé et de la sciure de bois. *Revue des sciences de l'eau / Journal of Water Science*, 31(2):109–126. DOI:<https://doi.org/10.7202/1051695ar>.
- Mekky, A.E.M., El-Masry, M.M., Khalifa, R.E., Omer, A.M., Tamer, T.M., Khan, Z.A., Gouda, M, and Mohy E.M.S. 2020. Removal of methylene blue dye from synthetic aqueous solutions using dimethylglyoxime modified amberlite IRA-420: kinetic, equilibrium and thermodynamic studies. *Desalination and Water Treatment*, 181: 399-411. DOI : 10.5004/dwt.2020.25097.
- Mobalaji, M.J., Olatunde, S.D., and Joshua, N.E. 2021. Sequestration of hazardous dyes from aqueous solution using raw and modified agricultural waste. *Adsorption Science and Technology*, 2021:1-21. DOI: <https://doi.org/10.1155/2021/6297451>.
- Musah, B.M., Peng, L., and Xu, Y. 2020. Adsorption of methylene blue using chemically enhanced *Platanus orientalis* leaf powder : kinetics and mechanisms. *Nat. Env. & Poll. Tech.*, 19 (1): 29-40. www.neptjournal.com.
- Nadew, T.T., Keana, M., Sisay, T., Getye B., and Habtu, N.G. 2023. Synthesis of activated carbon from banana peels for dye removal of an aqueous solution in textile industries: optimization, kinetics, and isotherm aspects. *Water Practice and Technology*, 18(4): 947-966. DOI: <https://doi.org/10.2166./wpt.2023.042>
- Narayana, S.K.V., and Ravi, V.K. 2019. Adsorption isotherm studies on methylene blue dye removal using naturally available biosorbent. *Rasayan J. Chem.*, 12(4): 2176-2182. DOI :<http://dx.doi.org/10.31788/RJC.2019.1245478>.
- Nigist, A.H., Ali, S.R., and Zemene, W.N. 2022. Chemical modification of neem (*Azadirachta indica*) biomass as bioadsorbent for removal of Pb²⁺ ion from aqueous wastewater. *Adsorption Science & Technology*, 2022: 18. DOI :<https://doi.org/10.1155/2022/7813513>.
- Nyakairu, G.W.A., Kapanga, P.M., Ntale, M , Lusamba, S.N., Tshimanga, R.M., Ammari, A. and Shehu, Z. 2024. Synthesis, characterization and application of Zeolite/Bi₂O₃ nanocomposite in removal of Rhodamine B dye from wastewater. *Cleaner Water*, 1(2024) :100004. DOI: <https://dx.doi.org/10.1016/j.clwat.2024.100004>.
- Pathania, D., Sharma, S., and Singh, P. 2017. Removal of methylene blue by adsorption onto activated carbon developed from *Ficus carica* bast. *Arabian journal of chemistry*, 10: S1445-S1451. DOI: <https://dx.doi.org/10.1016/j.arabjc.2013.04.021>.
- Rahimian, R., and Zarinabadi, S. 2020. A review of studies on the removal of methylene blue dye from industrial wastewater using activated carbon adsorbents made from Almond Bark. *Prog. Biochem. Res.*, 3(3) : 251-268. DOI : 10.33945/PCBR.2020.3.8.
- Raiyyaan, G.D., Khalith, M.S.B., Sheriff, A.M. and Arunachalam, K.D.A. 2021. Bio-adsorption of methylene blue dye using chitosan-extracted from *Fenneropenaeus indicus* shrimp shell waste, *J. Aquac. Mar. Biol.*, 10 (4): 146-150. <https://medcraveonline.com>.

- Razia, S., Syed, N.T., Usman, T.S., Yunus, K.T.M., Shaik, D.A.K., Imran, M., Kiran, S.M.A., Kalam, M.A., Ananda, M.H.C. and Akheel, A.S. 2022, Adsorption of Crystal Violet dye from aqueous solution using industrial pepper seed spent: Equilibrium, Thermodynamic, and Kinetic Studies. *Adsorption Science & Technology*, 2022: ID9009214. DOI:<https://doi.org/10.1155/2022/9009214>.
- Saad, T.M., Salah, O.H., Hussein, T.K., Ahjel, S., Abas, R.R., Alzahraa, Z.H., Muftun, N.F.M., and Omram A.A. 2024. Grass waste: A highly biosorbent for the removal of malachite green dye from aqueous solution. *Arabian Journal of Green Chemistry*, 8 (3): 349-359. DOI: 10.48309/AJGC.2024.449167.1489.
- Thiene, B.W., Kifuani, K.M., Kifuani, A.K.M., Ngoy, P.B., and Ekoko, G.B. Adsorption of a basic dye methylene blue in aqueous solution on a bioadsorbent from agricultural waste of *Manihot esculenta* Crantz. 2024. *Int. J. Biol. Chem. Sci.*, 18 (3): 1180-1198. DOI: <https://dx.doi.org/10.4314/ijbcs.v18i3.35>.
- Vanessa, P.V., Andrin, A., Le B.M., Lacombe, S., Frayret, J., and Pigot, T. 2017. Couplage photocatalytique-oxydation par le ferrate-VI pour le traitement du colorant Rhodamine 6G. *Revue des Sciences de l'eau*, 30(1):35-39. DOI: <https://dx.doi.org/10.7202/104006Lar>.
